

Optical bandpass switching by modulating a microcavity using ultrafast acousticsT. Berstermann,¹ C. Brüggemann,¹ M. Bombeck,¹ A. V. Akimov,^{2,3} D. R. Yakovlev,^{1,3} C. Kruse,⁴ D. Hommel,⁴ and M. Bayer¹¹*Experimentelle Physik 2, Technische Universität Dortmund, D-44227 Dortmund, Germany*²*School of Physics and Astronomy, University of Nottingham, Nottingham NG7 2RD, United Kingdom*³*A.F. Ioffe Physical-Technical Institute, Russian Academy of Sciences, 194021 St. Petersburg, Russia*⁴*Institut für Festkörperphysik, Abteilung Halbleitertechnik, Universität Bremen, 28359 Bremen, Germany*

(Received 29 September 2009; revised manuscript received 19 January 2010; published 12 February 2010)

We present time-resolved reflectivity spectra of the cavity mode in a II-VI semiconductor based planar microcavity that is modulated by a strain pulse injected using an ultrafast acoustics technique. The modulation occurs when the strain pulse passes interfaces of the layered cavity structure at which the electric field has an antinode. Maximum modulation is reached when the pulse enters or leaves the central cavity layer. The mode shifts in the cavity with a finesse of about 2000 are comparable to its mode linewidth, which shows that the proposed technique is prospective for ultrafast optical switching.

DOI: [10.1103/PhysRevB.81.085316](https://doi.org/10.1103/PhysRevB.81.085316)

PACS number(s): 78.20.hb, 78.67.Pt

I. INTRODUCTION

Miniaturized photonic resonator structures have attracted interest recently because of their huge potential for both fundamental science and technological applications. They may be used as passive filters selecting particular light wavelengths or to modify the light-matter interaction if an optically active medium is placed in the resonator.¹ An attractive system is a planar microcavity, consisting of a cavity layer sandwiched between two distributed Bragg reflectors (DBRs). Due to the atomic precision of epitaxial techniques, very high quality factors up to $\sim 10^5$ can be reached for these resonators, resulting in spectrally sharp confined photon modes surrounded by stop bands with close-to-unity reflectivity providing a sharp optical bandpass.²

Particularly interesting would be the possibility to modulate the optical dimensions of the microcavity. In that way, the energy of the cavity mode could be varied, which may be used for transparency switching in filter applications as well as for modulating the coupling of photons with emitting centers in the cavity (e.g., quantum dots or rare-earth ions). Such applications could turn out to be useful in optoelectronics and nanophotonics.

For quasistationary modulation, piezoelectric elements have been successfully used. For achieving the MHz frequency ranges, ultrasonic techniques are known to be very efficient for modulating the dimensions of periodic structures.^{3,4} However, reaching the subterahertz ($\sim 10^{10}$ – 10^{11} Hz) and terahertz (THz) frequency range is still a challenge. Here we investigate the potential that the methods of ultrafast acoustics offer for reaching ultrafast modulation. An introduction to picosecond acoustics techniques and corresponding references can be found in Ref. 5. Among the experiments in which these methods have been applied are studies of the elastic properties of layered nanostructures,^{6–11} generation of THz radiation¹² and ultrafast control of optical resonances in nanostructures.¹³

In contrast to our earlier works,^{14–17} where the investigated effects are based on the deformation-potential interaction of a strain pulse with a quantum well exciton embedded

in different structures, in this work we present experiments in which we apply the ultrafast acoustics methods to a semiconductor microcavity as a reliable and high quality photonic object. We show that the cavity mode energy can be changed by values up to ~ 1 meV within tens of picoseconds.

II. SAMPLE AND EXPERIMENT

A scheme of the experimental configuration and the sample structure is shown in Fig. 1(a). The central ZnSSe layer of the studied λ cavity has a size of 196 nm, corresponding to the targeted wavelength of the cavity mode. It is sandwiched between two DBRs formed by periodic stacks consisting of 18.5 (on the substrate side) and 15 (on the surface side) pairs of $\lambda/4$ layers of high (ZnSSe) and low (MgS/ZnCdSe superlattice) refractive index materials. Details about the design of the microcavity can be found in Ref. 18. The sample was grown on a 400 μm thick GaAs substrate. The λ -cavity contains also three ZnCdSse quantum wells around the central antinode position of the confined light field. However, at cryogenic temperatures, there is a 50 meV detuning of the quantum well exciton resonances to higher energies relative to the cavity mode,¹⁹ so that quantum well states do not need to be considered for the present experiments. In particular, polaritonic effects, such as reported in Refs. 15 and 16, are negligible. A reflectivity spectrum of the cavity at $T=10$ K is provided in Fig. 1(b) showing the cavity mode at the energy $E_0=2.470$ eV. The spectral linewidth of the cavity mode is $\delta E=1.2$ meV, leading to a quality factor $Q=E_0/\delta E\sim 2000$.

On the backside of the substrate, a 100-nm-thick aluminum film was deposited after polishing the substrate down to a thickness of 100 μm . The film serves as transducer for injection of the picosecond displacement pulses into the GaAs substrate [see Fig. 1(a)]. These pulses are generated by hitting the transducer with 150 fs short laser pulses (central wavelength 800 nm) emitted at a repetition rate of 100 kHz by a regenerative amplifier. The average power incident on the sample did not exceed 130 mW. A picosecond displacement pulse is injected into the semiconductor substrate due

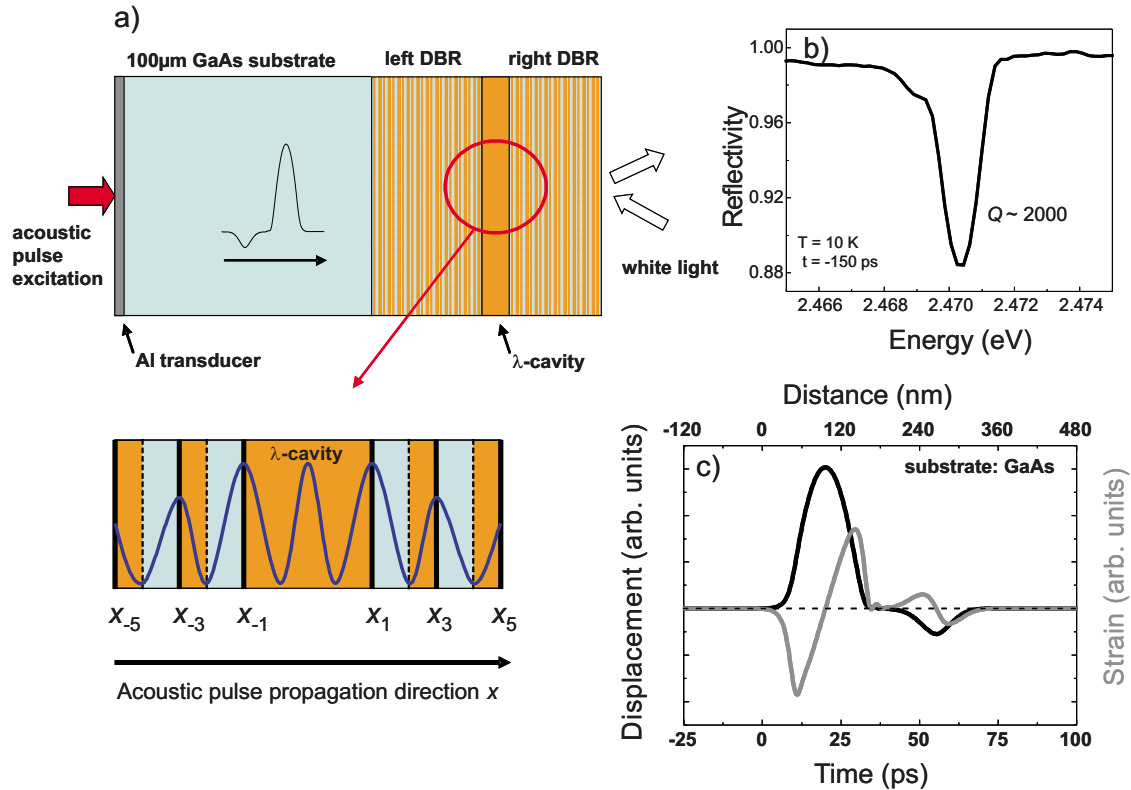


FIG. 1. (Color online) (a) Scheme of the experimental setup and sample structure consisting of the aluminum transducer, the GaAs substrate, and the cavity, sandwiched between two Bragg mirrors. The indicated interfaces correspond to the antinodes of the confined electric field (modulus sketched by blue solid curve) as described in the text. The displacement pulse is injected via a laser pulse, indicated as an arrow at the left side. Right arrows show the white laser pulses for probing the reflectivity spectrum. (b) Reflectivity spectrum from the microcavity structure without influence of the displacement pulse. (c) Typical temporal and spatial shapes of the displacement pulse (black line) and the corresponding strain (gray line) during propagation through the sample. Dashed line indicates zero displacement or strain.

to fast thermal expansion of the Al film after each excitation.^{13,20} This pulse, consisting of a coherent acoustic wave packet, propagates through the substrate with the longitudinal speed of sound ($v_{LA}=4800$ m/s in GaAs) such that it reaches the cavity structure after a propagation time $\tau_0 \approx 20$ ns. The performance of the experiment in a cryogenic environment ensures that damping of the acoustic wave packet due to anharmonic interaction with thermal phonons is negligible.²¹ The experiments were done out in a cryostat in which the sample was efficiently cooled by helium vapor. The temperature was measured by a sensor near the sample and stabilized at $T=10$ K using a manostat. No temperature rise under optical pump excitation was observed.

Figure 1(c) shows a typical temporal profile of a displacement pulse and the accompanying strain propagating in the GaAs substrate calculated according to Ref. 17. The dominant part of the displacement pulse can be well modeled by a Gaussian function. The small negative dip at 55 ps corresponds to a displacement resulting from internal reflections in the Al film. The displacement amplitude is on the order of picometer for typical optical excitation densities P (1–10 mJ/cm²) on the transducer, where the strain amplitude is 10^{-4} – 10^{-3} . The duration of the leading part of the pulse is about 20 ps which corresponds to a spatial extension of ~ 100 nm. The heat pulse generated in the metal film in

parallel with the displacement pulse is known to reach the opposite side of the substrate later than the coherent pulse²² so that it does not have to be considered here.

After passing the GaAs substrate, the acoustic pulse first reaches the left DBR of the microcavity [see Fig. 1(a)], then enters the central layer before reaching the right DBR. The idea of the experiment is to measure the effect of the acoustic pulse on the optical spectrum of the microcavity. This is realized by recording the spectral reflectivity spectrum using white light pulses originating from the same laser that excites the acoustic pulses in the transducer. The white light is generated by splitting off a part of the pulse emitted by the regenerative amplifier and sending it through a sapphire crystal. The white light pulse is reflected from the microcavity at variable time delays t with sampling steps of 300 fs.

III. EXPERIMENTAL RESULTS

Figure 2 shows a contour plot of experimentally measured reflectivity spectra as a function of the delay time when a laser pulse with an energy density of 6 mJ/cm² per pulse hits the transducer. We have defined $t=0$ shown by the dashed vertical line as the time when the maximum of the displacement profile of the pulse passes the middle of the cavity (at 6 mJ/cm²), which will be justified in the discussion part of this paper. At times well before $t=0$, the spec-

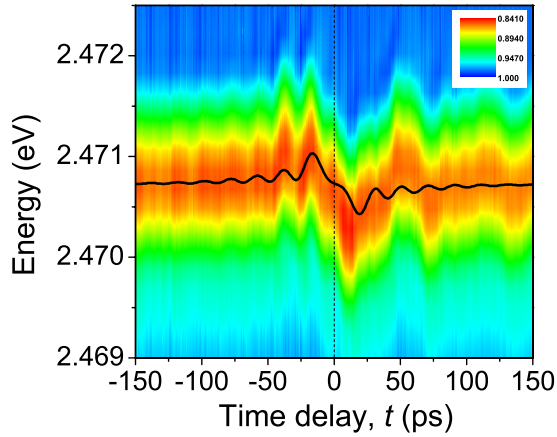


FIG. 2. (Color online) Spectral/temporal contour plot of the reflectivity in presence of the displacement pulse propagating through the structure measured at a laser energy density of $P=6$ mJ/cm² on the transducer ($T=10$ K). Black line shows the transfer-matrix calculation of the time evolution of the resonance mode energy for a Gaussian-shaped displacement pulse propagating with a velocity of 5365 m/s. Vertical dashed line indicates the time, when the middle of the cavity is maximum displaced.

trum consists of the cavity mode, which for delays up to $t=-150$ ps basically undergoes no changes, showing that the acoustic pulse does not yet influence the microcavity within the experimental accuracy. At later times, a modulation of the cavity mode is seen, which continuously becomes more pronounced up to $t\sim-20$ ps and shows a quasiperiodic temporal structure with repeated shifts toward higher energies compared to the unperturbed case. Maxima of the resonance energy modulation are reached at times, which are equidistantly spaced with a separation of 20 ps. The amplitude of the higher energy shifts has its maximum for the modulation peak at $t\approx-20$ ps and is equal to $\Delta E=0.28$ meV. For later times $t>0$, the mode shifts to lower energies by comparable amplitudes, but the temporal evolution of the modulation becomes more complicated and in particular the quasiperiodicity is lost.

Figure 3(a) shows the corresponding reflectivity plot for the signal measured at twice higher excitation density P . The modulation of the resonance energy to higher energies is stronger and reaches a maximum of $\Delta E=0.47$ meV, but the oscillations at $t<0$ are not so pronounced as at lower excitation density [compare Figs. 2 and 3(a)]. The inset in Fig. 3(b) shows the dependence of the maximum high energy shift ΔE on P . It is seen that for $P<9$ mJ/cm², this dependence is linear while at higher P saturation occurs.

IV. DISCUSSION

To understand the temporal-spectral behavior of the reflectivity signal, one has to consider (i) the changes of the cavity mode energy E_0 induced by the displacement of the interfaces in the Bragg mirrors and (ii) how E_0 changes with the strain induced modification of the refractive indices in the respective layers. At first we discuss the results on a qualitative level and then compare the temporal-spectral evo-

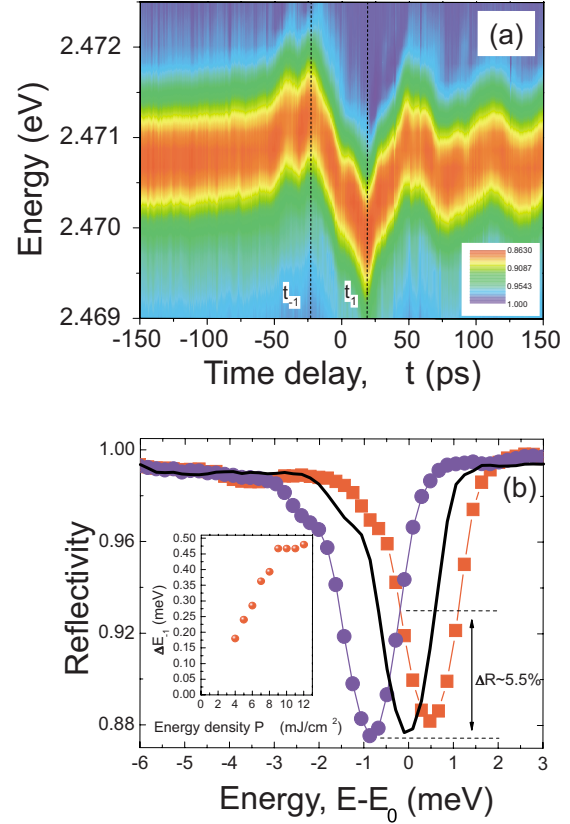


FIG. 3. (Color online) (a) Spectral/temporal contour plot of the reflectivity in the presence of the displacement pulse measured at a laser energy density of $P=12$ mJ/cm² on the transducer ($T=10$ K). (b) Three spectral cuts in panel (a) corresponding to the delay times $t_{-1}=-23$ ps (red squares), $t=-150$ ps (thick solid line), and t_1 (blue circles). (Inset) Dependence of the maximum higher energy shift ΔE_{-1} on the excitation laser energy P .

lution to calculations based on a transfer-matrix formalism.

While moving through the interfaces of the DBRs, the displacement pulse perturbs the periodicity of the structure by modulation of the interface positions x_i [see Fig. 1(a)], leading to modulation of E_0 . Apparently, if the modulation amplitude Δx_i is not too large ($0<|\Delta x_i|\ll\lambda$), displacements of the interfaces where the electric field has antinodes change E_0 , while the modulation of other interfaces where the electric field possesses nodes has negligible effect on E_0 . In the studied λ cavity, the field has antinodes in the center and also at the edges of the central cavity layer¹ [sketched by the red curve in the lower part of Fig. 1(a)]. Thus the displacement of these edge interfaces [$i=1$ and $i=-1$ on Fig. 1(a)] will have the biggest effect on E_0 . The displacement pulse, which is propagating along the x direction from left to right, reaches the left edge of the cavity layer ($i=-1$) and induces a positive displacement ($\Delta x_{-1}>0$). This corresponds to a compression of the cavity layer and correspondingly to an increase of E_0 . Later, the displacement pulse reaches the right cavity edge ($i=1$), inducing positive displacement of the interface ($\Delta x_1>0$). This leads to tension of the cavity layer and E_0 decreases. Qualitatively, such behavior is consistent with the experimental data presented in Figs. 2 and 3(a). There, the energy shifts with $\Delta E>0$ and $\Delta E<0$ are observed at $t<0$ and $t>0$, respectively.

The displacements of the uneven interfaces inside the DBRs ($i = \pm 3, \pm 5, \dots$) at which the electric field possesses antinodes also affect E_0 . These interfaces are marked by bold solid lines in Fig. 1(a) and correspond to refractive index changes from low to high along the x direction. The influence of Δx_i on E_0 in the DBRs will decrease with increasing distance of the respective interface from the cavity edges because the electric field is decaying exponentially inside the DBRs. The penetration depth of the light field into the DBRs is calculated to be 420 nm,¹ corresponding to about twice the wavelength of the cavity. Thus, when the displacement pulse moves through the left DBR from left to right, the effect of Δx_i on E_0 will appear as high energy shifts with amplitude $\Delta E_i > 0$ at the temporal positions t_i when the pulse passes the corresponding interface. The value of ΔE_i increases when the pulse approaches the central layer. In the right DBR, the process evolves in reversed order, so that $\Delta E_i < 0$ decreases when the pulse moves away from the cavity layer. The observation of the quasiperiodic oscillations in the experimentally measured temporal evolution of E_0 (Fig. 2) while the displacement pulse passes the left DBR is also in agreement with this qualitative consideration.

Similarly, it is possible to include on a qualitative level the effect of strain-induced changes in the refractive index. Taking into account the sign of the elasto-optical constant,²³ it is easy to show that this contribution causes shifts of the cavity resonance energy E_0 in the same direction as the displacement of the interfaces.

To be more specific, we have performed calculations of the cavity mode energy in the presence of a moving Gaussian displacement pulse, corresponding to the dominant part of the pulse shown in Fig. 1(c), using a transfer-matrix formalism. The result for the displacement amplitude 0.04 nm, corresponding to a strain amplitude of 0.7×10^{-3} , is shown in Fig. 2 by the solid line. For a sound velocity of 5365 m/s in the DBR, good agreement between the experiment and calculations is seen in the time interval when the displacement pulse passes the left DBR and the cavity layer. The calculations confirm the main point of the qualitative discussion that the resonance energy changes only when the acoustic pulse passes the interfaces where the electric field possesses antinodes. At later times, when the displacement pulse is propagating through the right DBR, the experimentally measured signal behaves different from the one predicted theoretically. This discrepancy apparently is due to a more complex displacement pulse time evolution in comparison to the simple Gaussian shape used in the model. Indeed, the layered structure of the microcavity will cause multiple hypersonic reflections at the interfaces resulting in oscillating features in the tail of the displacement pulse.¹⁶

Now we turn to the discussion of the experimental result obtained for high values of P (Fig. 3). The value of the maximum positive resonance energy shift ΔE_{-1} saturates at high excitation density [Fig. 3(b) inset] and the oscillations of ΔE_i (x_{-3}, x_{-5}, \dots) are less pronounced than for low P [compare Figs. 2 and 3(a)]. Such a behavior is the result of nonlinear propagation when the acoustic pulse propagates through the GaAs substrate. It is well known that at high P (i.e., high displacement and strain amplitudes), the initially injected Gaussian pulse spreads in time while the corre-

sponding strain is transformed into a shock wave front, acoustic solitons, and a dispersive tail.^{17,24} Thus, at high P , the displacement pulse possesses a complex temporal shape covering more than one interface and correspondingly the oscillatory behavior of E_0 becomes less pronounced. The spatial spreading of the displacement pulse with increase of P also explains the saturation of ΔE_{-1} at high densities [inset of Fig. 3(b)]. Furthermore, the complicated pulse shape can lead to the fact that the maximum of the lower energy shift $\Delta E_1 = -0.8$ meV at $t_1 = 19$ ps appears to be notably larger than ΔE_{-1} at $t_{-1} = -23$ ps at high excitation densities. This difference can be seen in Fig. 3(b) where corresponding cuts through the reflectivity spectra are shown. Indeed, spreading of the negative and positive displacement parts of the pulse over the left and right DBRs will induce bigger shifts of E_0 in comparison to those induced by a Gaussian-shaped pulse or an asymmetric strain profile.

The maximum measured cavity mode energy shift from higher to lower energy is equal to 1.3 meV which is comparable to the cavity mode spectral width of 1.2 meV. This can be seen in Fig. 3(b), which shows spectral cuts of Fig. 3(a) at t_{-1} (red squares) and t_1 (blue circles). The cut at $t = -150$ ps (thick solid line) corresponds to an energy of the cavity mode, which is not yet affected by the displacement pulse. Taking into account the resonance width, the observed reflectivity change is 5.5% at an energy exceeding (being equal) the width of the cavity mode. This corresponds to a change in transmission of 50% for negligible absorption.

The switching energy density P per excitation laser pulse on the metal transducer, which is necessary to shift the cavity mode frequency by a value exceeding the resonance linewidth, thereby is equal to 12 mJ/cm². This value may be easily reached using moderate focusing of a 1 μ J laser pulse and might be reached even with a ~ 1 nJ pulse by tightly focusing the laser beam on the metal transducer.²¹

The measured energy shift of the optical resonance ~ 1 meV is comparable to the values for the resonance energy shift in GaAs-based microcavities with embedded quantum wells.^{15,16} In these works, the explanation of the observed effects was based on a deformation-potential mechanism which strongly influences the energy of the quantum well exciton involved in the formation of polaritons. No evidence of strong changes in these polariton resonances, which show the avoided crossing of coupled resonances, was observed before the strain pulse reached the central cavity layer. Thus, strain-induced effects on the refractive indices and the cavity layer dimensions were ignored in Refs. 15 and 16 as we supposed them to be small compared to the effects governed by the energy modulation of the exciton resonance. This difference in observations compared to the present work most likely arises from the different response of III-V and II-VI semiconductor cavities to the strain pulse. In particular, the II-VI system investigated here is expected to show an increased response to an acoustic pulse due to the reduced layer thicknesses in the cavity stack sequence relative to the strain pulse extension as compared to the corresponding ratio in the III-V systems of Refs. 15 and 16.

V. SUMMARY AND OUTLOOK

We have demonstrated that the cavity mode energy is changed within tens of picoseconds when a displacement

pulse moves mirror interfaces close to the central layer of the λ cavity at which the confined light field takes its maxima. An oscillatory behavior of the cavity resonance energy is observed. The signals measured in this work are induced by processes which were not reported in earlier works where the oscillatory behavior of the probe intensity was observed.²⁵ The reported results open many possibilities. The obvious and attractive one is ultrafast modulation of the filtering function of a resonator. If the layer contains an active medium such as quantum dots, it may allow one to load particular dot structures by optically excited carriers and keep these dots excited until the next modulation creates again a resonance with the optical mode energy. For these applications, one may increase the Q value of the resonator by 1 order of magnitude to perform a complete ps switch, offering the possibility of ultrafast gating. The characteristic time dependence of the switch might be tailored by controlling the shape and the spatial extension of the displacement pulse using acoustic filters and/or alternative metal transducers. In

this respect, combination of optical and acoustic microcavities may be a step forward to THz modulation of light. But also for fundamental quantum effects resonator modulation may turn out to be attractive. High quality resonators may also be formed by a Bragg mirror and a metal tip that is positioned close to the Bragg mirror by a piezodrive. In such a resonator, huge field enhancements may be obtained, whose amplitude may be modulated through modulation of the Bragg mirror. Further, the investigation of the dynamical Casimir effect based on the action of fast oscillating cavity boundaries on the vacuum field might be a prospective application.²⁶

ACKNOWLEDGMENTS

We are thankful to P. J. S. van Capel for providing simulation results on nonlinear acoustics. This work has been supported by the Deutsche Forschungsgemeinschaft (Grant No. BA1549/14-1).

-
- ¹A. V. Kavokin, J. J. Baumberg, G. Malpuech, and F. P. Laussy, *Microcavities* (Oxford University Press, New York, 2008).
- ²S. Reitzenstein, C. Hofmann, A. Gorbunov, M. Strauß, S. H. Kwon, C. Schneider, A. Löffler, S. Höfling, M. Kamp, and A. Forchel, *Appl. Phys. Lett.* **90**, 251109 (2007).
- ³M. M. de Lima, Jr. and P. V. Santos, *Rep. Prog. Phys.* **68**, 1639 (2005).
- ⁴D. Gérard, V. Laude, B. Sadani, A. Khelif, D. Van Labeke, and B. Guizal, *Phys. Rev. B* **76**, 235427 (2007).
- ⁵http://en.wikipedia.org/wiki/Picosecond_ultrasonics
- ⁶J. J. Baumberg, D. A. Williams, and K. Köhler, *Phys. Rev. Lett.* **78**, 3358 (1997).
- ⁷A. Bartels, T. Dekorsy, H. Kurz, and K. Köhler, *Appl. Phys. Lett.* **72**, 2844 (1998).
- ⁸C.-K. Sun, J.-C. Liang, and X.-Y. Yu, *Phys. Rev. Lett.* **84**, 179 (2000).
- ⁹A. J. Kent, R. N. Kini, N. M. Stanton, M. Henini, B. A. Glavin, V. A. Kochelap, and T. L. Linnik, *Phys. Rev. Lett.* **96**, 215504 (2006).
- ¹⁰M. F. Pascual Winter, G. Rozas, A. Fainstein, B. Jusserand, B. Perrin, A. Huynh, P. O. Vaccaro, and S. Saravanan, *Phys. Rev. Lett.* **98**, 265501 (2007).
- ¹¹N. D. Lanzillotti-Kimura, A. Fainstein, A. Huynh, B. Perrin, B. Jusserand, A. Miard, and A. Lemaître, *Phys. Rev. Lett.* **99**, 217405 (2007).
- ¹²M. R. Armstrong, E. J. Reed, K.-Y. Kim, J. H. Glownia, W. M. Howard, E. L. Piner, and J. C. Roberts, *Nat. Phys.* **5**, 285 (2009).
- ¹³O. B. Wright, *Phys. Rev. B* **49**, 9985 (1994).
- ¹⁴A. V. Akimov, A. V. Scherbakov, D. R. Yakovlev, C. T. Foxon, and M. Bayer, *Phys. Rev. Lett.* **97**, 037401 (2006).
- ¹⁵A. V. Scherbakov, T. Berstermann, A. V. Akimov, D. R. Yakovlev, G. Beaudoin, D. Bajoni, I. Sagnes, J. Bloch, and M. Bayer, *Phys. Rev. B* **78**, 241302(R) (2008).
- ¹⁶T. Berstermann, A. V. Scherbakov, A. V. Akimov, D. R. Yakovlev, N. A. Gippius, B. A. Glavin, I. Sagnes, J. Bloch, and M. Bayer, *Phys. Rev. B* **80**, 075301 (2009).
- ¹⁷A. V. Scherbakov, P. J. S. van Capel, A. V. Akimov, J. I. Dijkhuis, D. R. Yakovlev, T. Berstermann, and M. Bayer, *Phys. Rev. Lett.* **99**, 057402 (2007).
- ¹⁸C. Kruse, S. M. Ulrich, G. Alexe, E. Roventa, R. Kröger, B. Brendemühl, P. Michler, J. Gutowski, and D. Hommel, *Phys. Status Solidi B* **241**, 731 (2004).
- ¹⁹R. Granger, J. T. Benhlal, O. Ndad, and R. Triboulet, *Eur. Phys. J. B* **13**, 429 (2000).
- ²⁰G. Tas and H. J. Maris, *Phys. Rev. B* **49**, 15046 (1994).
- ²¹H.-Y. Hao and H. J. Maris, *Phys. Rev. B* **63**, 224301 (2001).
- ²²B. Perrin, E. Péronne, and L. Belliard, *Ultrasonics* **44**, e1277 (2006).
- ²³B. H. Bairamov, A. V. Gol'tsev, V. V. Toporov, R. Laiho, and T. Levola, *Phys. Rev. B* **33**, 5875 (1986).
- ²⁴O. L. Muskens and J. I. Dijkhuis, *Phys. Rev. B* **70**, 104301 (2004).
- ²⁵O. Matsuda and O. B. Wright, *J. Opt. Soc. Am. B* **19**, 3028 (2002).
- ²⁶G. T. Moore, *J. Math. Phys.* **11**, 2679 (1970).